

# Free Energy of Amide Hydrogen Bond Formation in Vacuum, in Water, and in Liquid Alkane Solution

Nir Ben-Tal,<sup>†</sup> Doree Sitkoff,<sup>§</sup> Igor A. Topol,<sup>‡</sup> An-Suei Yang,<sup>†</sup> Stanley K. Burt,<sup>‡</sup> and Barry Honig<sup>\*,†</sup>

Department of Biochemistry and Molecular Biophysics and Center for Biomolecular Simulation, Columbia University, 630 West 168th Street, New York, New York 10032, and Structural Biochemistry Program, Frederick Biomedical Supercomputing Center, SAIC Frederick, National Cancer Institute-Frederick Cancer Research and Development Center, Frederick, Maryland 21702

Received: June 19, 1996; In Final Form: October 10, 1996<sup>®</sup>

The energy of dimerization of two *N*-methylacetamide (NMA) molecules in vacuum is calculated using density functional theory. Natural orbital analysis suggests that the dimerization energy of  $-6.6$  kcal/mol is predominantly due to the  $(\text{N}-\text{H}\cdots\text{O}=\text{C})$  donor–acceptor interaction. The gas phase to water hydration free energies and the free energies of transfer from the aqueous phase to liquid alkane of hydrogen bonded,  $(\text{N}-\text{H}\cdots\text{O}=\text{C})$ , and nonbonded,  $(\text{N}-\text{H},\text{O}=\text{C})$ , groups are calculated using a continuum solvent model. On the basis of these calculations, we estimate the free energy of forming an amide hydrogen bond in the context of the NMA dimer in water and in liquid alkane as  $\sim -1$  and  $\sim -5$  kcal/mol, respectively. The relevance of these calculations to processes such as protein folding and membrane insertion of proteins is discussed.

## 1. Introduction

Hydrogen bonding is known to play a key role in determining the structure of proteins in aqueous solutions and in lipid bilayers.<sup>1–5</sup> The importance of the peptide backbone hydrogen bond has motivated the study of similar hydrogen bonds in small amides. The first estimate of the energies associated with forming an amide hydrogen bond in aqueous phase was carried out by Schellman, using osmotic pressure and heat of dilution data on urea.<sup>6,7</sup> Subsequent values for hydrogen bond formation energies in polar and organic solvents,  $\Delta G_4$  and  $\Delta G_7$  in Figure 1, respectively, have been obtained by related approaches, i.e., measuring the binding constants of small molecules capable of forming amide hydrogen bonds<sup>8–20</sup> and manipulating these experimental values to extract the relative contribution of the hydrogen bond.<sup>21,22</sup> Hydrogen bond energies have also been calculated by mutating hydrogen bonding partners in proteins and measuring the resultant effects on protein stability.<sup>23–25</sup> Estimates for the free energy of transfer of hydrogen bonded  $(\text{N}-\text{H}\cdots\text{O}=\text{C})$  and nonbonded  $(\text{N}-\text{H},\text{O}=\text{C})$  groups between polar and organic solvents,  $\Delta G_6$  and  $\Delta G_5$  in Figure 1, respectively, have been obtained on the basis of measurements of the partition of *N*-methylacetamide, NMA, molecules between polar and organic solvents and the dimerization energy in these solvents.<sup>26,27</sup> Additionally, several recent studies have used computational techniques, such as Monte Carlo<sup>28</sup> or molecular dynamics<sup>29</sup> simulations and continuum solvent models,<sup>30,31</sup> to calculate the energy of hydrogen bond formation between small polar molecules.

The results of these studies are qualitatively similar in certain respects: the energetic penalty associated with transferring the unassociated hydrogen bonding groups from water to a low dielectric solvent is consistently larger than the penalty of transferring the hydrogen bonded pair (i.e.,  $\Delta G_5 > \Delta G_6$ ), or equivalently, hydrogen bond formation is more favorable in

organic medium than in water (i.e.,  $\Delta G_7 < \Delta G_4$ ). Nevertheless, the estimated values for these processes vary widely; the reported energies associated with breaking a hydrogen bond in water range from  $-3.1^9$  to  $+6.2$  kcal/mol,<sup>22</sup> while the energy of hydrogen bond formation in a low dielectric solvent has been estimated at values ranging from  $-8.4^{29}$  to  $-0.9$  kcal/mol.<sup>9</sup> These uncertainties are reflected in the fact that it is not yet clear whether hydrogen bonds stabilize or destabilize proteins.<sup>2,17,23,32–35</sup>

A complicating factor in the interpretation of the literature is that the definition of hydrogen bond energy differs in the various studies. An experimentally measured energy of association between two molecules forming an  $\text{N}-\text{H}\cdots\text{O}=\text{C}$  hydrogen bond has many contributions. These include direct electrostatic interactions between the  $\text{N}-\text{H}$  and  $\text{C}=\text{O}$  groups, direct electrostatic interactions involving groups other than the hydrogen bonding pair, desolvation effects, translational and rotational entropic losses, and formation of new vibrational degrees of freedom. While some authors have considered the entire association energy of the two molecules as a measure of hydrogen bond formation,<sup>9,13,27</sup> others have attempted to subtract out contributions specific to the system under consideration, such as those due to neighboring groups<sup>26</sup> and translational and rotational entropy,<sup>22</sup> in order to arrive at a more universal measure of the hydrogen bond energetic contribution.

To complicate matters further, the procedures used to extract hydrogen bond energies from measured or calculated total energies of association or transfer are frequently controversial. For example, desolvation contributions from groups near the hydrogen bonded pair have been estimated using group contribution solvation approaches;<sup>21,26,27</sup> however, these methods neglect effects due to electrostatic interactions of neighboring groups, and moreover, different implementations of this approach have yielded different results. Several methods of estimating translational and rotational entropic contributions have been described in the literature, leading to a  $\sim 3$  kcal/mol uncertainty in hydrogen bonding energies by one calculation.<sup>22</sup>

Uncertainties in the structure of the hydrogen bonded pair add further difficulties to the interpretation of measured hydrogen bond values. For example, measured dimerization

<sup>†</sup> Columbia University.

<sup>‡</sup> Frederick Biomedical Supercomputing Center.

<sup>§</sup> Department of Molecular Biology, The Scripps Research Institute, 10666 N. Torrey Pines Road, La Jolla, CA 92037.

<sup>®</sup> Abstract published in *Advance ACS Abstracts*, December 1, 1996.

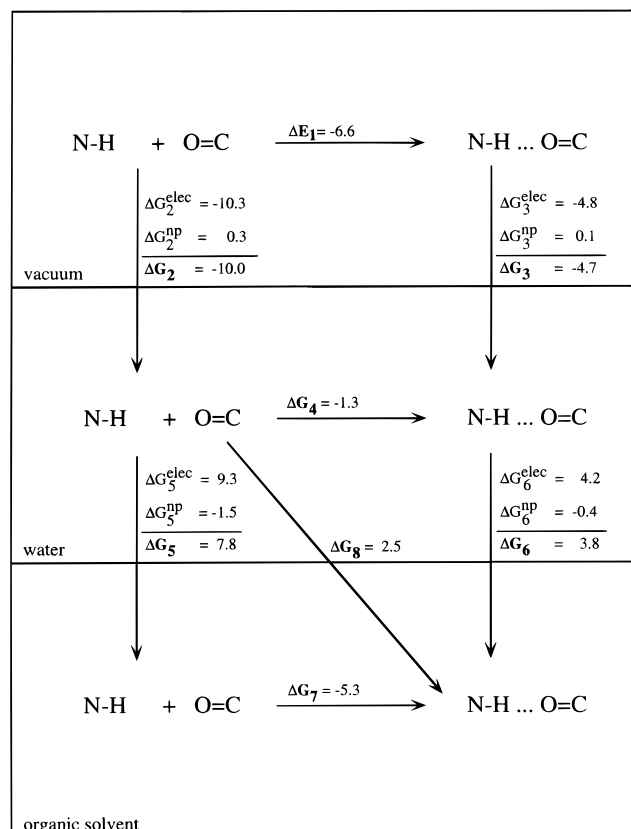


**Figure 1.** Thermodynamic cycle of hydrogen bond formation between N-H and O=C groups in different phases. Energy values were calculated for these groups in the context of the NMA dimer and where the organic solvent was hexane/cyclohexane, referred to as liquid alkane, as described in the text.

energies may include contributions from configurations near but not exactly in the geometry of minimum energy. In an extreme example of this problem, Monte Carlo simulations of the dimerization of NMA in water suggest that the molecules associate in a stacked rather than hydrogen bonded geometry, thus the measured value may have no relation to hydrogen bond energy whatsoever.<sup>28</sup>

In this paper, the energies of forming an amide hydrogen bond between two NMA molecules in aqueous phase and in hexane/cyclohexane, referred to as liquid alkane ( $\Delta G_4$  and  $\Delta G_7$  in Figure 1, respectively), are estimated as the sum of direct interactions between the hydrogen bonded pair in vacuum ( $\Delta E_1$ ), calculated quantum mechanically, and indirect solvent effects ( $\Delta G_2$ ,  $\Delta G_3$ ,  $\Delta G_5$ , and  $\Delta G_6$ ), calculated using a continuum solvent approach. The idea of estimating the hydrogen bonding energy between two NMA molecules as a sum of contributions from direct vacuum interaction and the effects of the solvent was used earlier by Simonson and Brunger.<sup>30</sup> The major differences between their scheme and ours is that they used a classical forcefield, X-PLOR,<sup>36</sup> for the direct interaction, while we use ab initio quantum mechanical calculations. In addition, while both studies calculate the dimerization energy of NMA, we also calculate the partial contributions of the N-H and C=O groups to the interaction. [The assumption in both studies is that the direct interaction is decoupled from the solvent effects. Warshel<sup>37</sup> suggests an alternative method, empirical valence bond, where the direct and indirect energy contributions for forming ion pairs during proton transfer reactions in enzymes in aqueous phase are coupled. It is possible to use the same method for studying hydrogen bonding as well.] In contrast to previous methods that used group additivity techniques for estimating the partial contribution of the N-H and C=O groups

to hydrogen bonding (e.g., refs 27 and 26), we calculate those contributions directly on the basis of the fundamental equations of electrostatics. The results indicate that, while amide hydrogen bonds are, at best, marginally stable in aqueous phase, they are very stable in liquid alkane. We also show that, in qualitative agreement with all of the available estimates, a much larger free energy penalty exists for transferring the nonbonded (N-H...O=C) group from aqueous phase to the organic solvent (liquid alkane in this study), compared to the bonded (N-H...O=C) group.

## 2. Theory and Methods

The thermodynamic cycle used in the calculation is shown in Figure 1: The association energy between two hydrogen bonding species in water,  $\Delta G_4$ , was estimated by summing their binding energy in vacuum,  $\Delta E_1$ , and the difference between the free energies of hydration of the hydrogen bonded (N-H...O=C) and nonbonded (N-H, O=C) groups,  $\Delta G_3$  and  $\Delta G_2$ , respectively.

$$\Delta G_4 = \Delta E_1 + \Delta G_3 - \Delta G_2 \quad (1)$$

The contribution of conformational entropy to the dimerization is not accounted for, as will be discussed below; hence we use internal rather than free energy in vacuum.

Similarly, the association energy between two hydrogen bonding species in liquid alkane,  $\Delta G_7$ , was estimated by summing their association free energy in water,  $\Delta G_4$ , and the difference between the water to liquid alkane solvation free energies of the hydrogen bonded (N-H...O=C) and nonbonded (N-H, O=C) groups,  $\Delta G_6$  and  $\Delta G_5$ , respectively.

$$\Delta G_7 = \Delta G_4 + \Delta G_6 - \Delta G_5 = \Delta E_1 - \Delta G_2 + \Delta G_3 - \Delta G_5 + \Delta G_6 \quad (2)$$

The free energy of forming a hydrogen bond in water and subsequently transferring it into organic solvent or, alternatively, transferring the nonbonded (N-H, O=C) group into organic solvent and subsequently forming a hydrogen bond, is given by

$$\Delta G_8 = \Delta G_4 + \Delta G_6 = \Delta G_5 + \Delta G_7 \quad (3)$$

In addition, we estimated the dimerization free energy of two NMA molecules in water and in liquid alkane from their dimerization energy in vacuum and the appropriate hydration/solvation free energies of NMA monomer and dimer. The thermodynamic cycle used in those calculations is presented in Figure 2. Each process in the cycle is given a Roman numeral according to the analogous process in the cycle of Figure 1 (e.g., the dimerization energy in vacuum, which is the analogue of the hydrogen bonding energy in vacuum,  $\Delta E_1$ , is denoted by  $\Delta E_I$ , etc.).

The vacuum phase dimerization energy of two NMA monomers to form a hydrogen bond,  $\Delta E_I$  of Figure 2, was calculated quantum mechanically and was used for estimating  $\Delta E_I$ . The hydration/solvation free energies ( $\Delta G_j$ ,  $j = 2, 3, 5, 6, \text{II}, \text{III}, \text{V}, \text{VI}$ ) were calculated using a continuum solvent model as will be described below.

**Molecular Structures.** An approximate geometry for the NMA monomer was constructed by building and energy minimizing in the gas phase with the CVFF forcefield<sup>38</sup> using the Insight/Discover molecular modeling program (MSI). To produce an approximate dimer structure, the NMA monomers were docked according to the minimum hydrogen bonding conformation observed in a previous ab initio calculations for the dimerization of a formamide and a formaldehyde molecule

in vacuum, i.e., the O–N distance was 2.9 Å and the N–H–C angle between the hydrogen bonded atoms was 138°. <sup>39</sup> The NMA monomer and dimer structures were subsequently minimized using the density functional theory (DFT) program DGauss (available as part of the UniChem software from Cray Research, Eagan, MN) with the DZVP2 basis set <sup>40</sup> to maximum force of 0.0005 hartree/Å. The N–O distance and the N–H–C angle in the minimized NMA dimer structure were 2.96 Å and 170.4°, respectively. The success of DFT methods in describing hydrogen bonded complexes is well documented; DFT is compatible with high-level post-Hartree–Fock methods and gives results within experimental error. <sup>41–47</sup> Basis set superposition error (BSSE) corrections, which have been estimated at less than 1 kcal/mol, <sup>44</sup> were not included. It has been shown that for weakly hydrogen bonded dimers BSSE in the DFT calculations is on the order of experimental uncertainty and the question whether BSSE should be used or ignored cannot be unequivocally resolved for those particular cases <sup>44</sup> (see also Dykstra <sup>48</sup>). A more detailed description of the procedure used for the minimization, as well as convergence tests with respect to different basis sets, and comparison with experimental values, has been given in Topol et al. <sup>44</sup> It has been concluded, on the basis of the comparison of experimental and calculated thermodynamic parameters, that the density functional approach yields rather accurate thermodynamics of hydrogen bonding.

NMA dimer conformations resembling those found in  $\alpha$ -helical and parallel and antiparallel  $\beta$ -sheet secondary structures in proteins were also built, using the geometry parameters given in Table IV in a recent paper by Mitchell and Price. <sup>39</sup> When the  $\alpha$ -helical conformation was subsequently geometry optimized in DGauss, it reverted to the minimum dimer structure obtained above; the preminimized dimer structure was therefore used in the thermodynamic energy cycle calculations. In contrast, the geometries of the optimized parallel and antiparallel  $\beta$ -sheet structures remained close to the initial structures; thus the optimized structures were used.

**Vacuum Phase Contributions (Steps 1 of Figure 1 and I of Figure 2).** The quantum mechanical internal energies of the geometry-optimized monomer and dimer structures were computed using the program DGauss with the same protocol used in the geometry optimization process. Twice the energy of the geometry-optimized monomer was subtracted from the energy of the geometry-optimized dimer, to yield the dimerization internal energy in vacuum,  $\Delta E_1$ . In the case of the NMA dimer in the  $\alpha$ -helical conformation, the energy of the initially generated, unminimized dimer structure was used, as mentioned above, and the energy contribution of the two (unminimized) NMA monomers was subtracted from this value.

The primary electron orbital contributions to the DGauss association energies of NMA dimer were computed using GAUSSIAN92 <sup>49</sup> natural orbital analysis. The procedure that was used has been described in detail in refs 50 and 51. On the basis of the results of the analysis (presented below), the full dimerization energy from the NMA hydrogen bonding process,  $\Delta E_1$  of Figure 2, was taken as an estimate for the (C=O...N–H) hydrogen bond energy in vacuum,  $\Delta E_1$  of Figure 1.

As a check of the calculated energies, the DGauss-minimized NMA monomer and dimer (in the overall energy minimum configuration) were reminimized using the quantum chemistry program PS-GVB, <sup>52,53</sup> with localized MP2 correlation and the cc-pVTZ basis set. <sup>54</sup> The difference in resultant energies of the monomers and dimer, –6.9 kcal/mol, is in excellent agreement with the result obtained from the DGauss density functional calculation, –6.6 kcal/mol.

**Hydration/Solvation Free Energy Contributions (Steps 2, 3, 5, and 6 of Figure 1 and II, III, V, and VI of Figure 2).** The free energies of transfer of the geometry-optimized NMA monomer and dimer (and the partial contribution of the hydrogen bonded and nonbonded groups to the free energies of transfer) in each of the processes 2, 3, 5, and 6 of Figure 1 (and their analogues of Figure 2) were calculated using the FDPB/ $\gamma$  method. <sup>55,56</sup> In this method, the free energy,  $\Delta G_j$ , ( $j = 2, 3, 5, 6, \text{II, III, V, VI}$ ), is a sum of electrostatic contributions,  $\Delta G_j^{\text{elect}}$ , obtained by finite difference solution to the Poisson equation (FDPB method), and nonpolar (cavity/van der Waals) contributions,  $\Delta G_j^{\text{np}}$ , which are added as a surface area dependent term, with a single surface tension coefficient ( $\gamma$ ) derived from partitioning of alkanes between different phases.

$$\Delta G_j = \Delta G_j^{\text{elect}} + \Delta G_j^{\text{np}} \quad (4)$$

**Electrostatic Solvation Free Energy Contribution,  $\Delta G_j^{\text{elect}}$ .** The electrostatic contributions to the free energies of transfer,  $\Delta G_j^{\text{elect}}$  ( $j = 2, 3, 5, 6, \text{II, III, V, VI}$ ), were calculated using a continuum representation of the solvents, following the approach which has been described in detail by Sitkoff et al. <sup>55,56</sup> The solute was represented as a collection of atomic centered partial charges embedded in a solute-shaped cavity, surrounded by a continuous dielectric solvent. Atomic radii were taken from the PARSE parameter set (see Table 4 of Sitkoff et al. <sup>55</sup>). The atomic charges for processes of transfer from vacuum to water, and water to liquid alkane (hexane or cyclohexane), were taken from Tables 3 of refs 55 and 56, respectively. These two sets of atomic charges and radii have been parametrized to reproduce experimentally measured hydration (vacuum to water) and solvation (water to liquid alkane) free energies of small molecules which are the side chains and backbone of the amino acids (including NMA), respectively. In concert with the suitable surface tension coefficients (see below) the two sets of atomic charges and radii reproduce vacuum–water and alkane–water solvation free energies with average absolute errors of 0.15 and 0.21 kcal/mol, respectively. <sup>55,56</sup>

To the best of our knowledge, there is no published value for the measured free energy of transfer of NMA from water to liquid alkane. Hence, we estimated this value on the basis of an empirical relationship that was recently found between small molecule hydration (vacuum to water) and water to liquid alkane transfer free energies, i.e., that the electrostatic contribution to water to liquid alkane solvation energy is –90% of the vacuum to water value. <sup>56</sup> The electrostatic contribution to the hydration free energy is –12.2 kcal/mol (Table 3 of Sitkoff et al. <sup>55</sup>). The electrostatic contribution to the water to liquid alkane transition is thus  $-0.9(-12.2) = 11.0$  kcal/mol by this empirical rule. The partial charges on the atoms of the NMA molecule were parametrized to reproduce this value. Adding the nonpolar contribution (using the water accessible area, as described below) of –4.8 kcal/mol, the total water to liquid alkane solvation free energy is 6.2 kcal/mol (see Figure 2). Recalling that liquid alkane is less polar than CCl<sub>4</sub>, it is encouraging to see that our value is larger than the water to CCl<sub>4</sub> free energy of transfer of this molecule, 4.1 kcal/mol, which was measured by Klotz and Farnham. <sup>27</sup>

The partial atomic charges for the NMA molecule for the water to liquid alkane transition were obtained by the same procedure used to derive atom charges for all the other molecules; by fitting simple bond dipole moments to functional groups in a manner that optimizes the agreement between calculated and experimental solvation free energies for molecules containing those groups. <sup>56</sup> The amide group was treated as a sum of ketone and amine groups. The appropriate charges for the ketone were the ones used for the fitting of acetone,

etc., and the amine group was taken from methylimidazole. Specifically, charges of +0.68 and -0.68, respectively, were chosen for C and O of the ketone group, and +0.45 and -0.45, respectively, were chosen for H and N of the amine group. The rest of the atoms were assigned a charge of zero. These charges, used in conjunction with the PARSE radii, yield a water to liquid alkane transfer free energy of 11 kcal/mol, in excellent agreement with the experimental value derived in the previous paragraph.

For the C=O,N-H electrostatic solvation free energy contributions (steps 2, 3, 5, and 6 in Figure 1), only the C, O, N, and H atoms in the NMA dimer which are involved in hydrogen bonding (and the same atoms on each of the two nonbonded monomers) were assigned partial charges; the rest of the groups were assigned a charge of zero.

The solvent dielectric was assigned to its appropriate value (i.e., 80 for room-temperature water, 1 for vacuum, 2 for liquid alkanes).<sup>57</sup> In accordance with previous work, to account for solute polarizability the solute dielectric was assigned to be 2, corresponding to the high-frequency dielectric constant of small molecules.<sup>58</sup> The boundary between solute and solvent ("molecular surface") is defined by the distance of closest approach of the surface of a solvent-sized molecule to the solute. The Poisson equation for the system

$$\nabla \cdot \epsilon(\vec{r}) \nabla \phi(\vec{r}) + 4\pi \rho(\vec{r}) = 0 \quad (5)$$

where  $\epsilon(\vec{r})$  is the dielectric constant,  $\rho(\vec{r})$  is the solute charge density, and  $\phi(\vec{r})$  is the electrostatic potential at point  $\vec{r}$ , was solved by first mapping the charge and dielectric information onto a three-dimensional lattice. The equation was then solved on the lattice in finite difference form<sup>59</sup> via an iterative algorithm,<sup>60</sup> using the program DelPhi.<sup>61</sup> The solution yields the electrostatic potential at every grid point.

The electrostatic solvation free energy,  $\Delta G_j^{\text{elect}}$  ( $j = 2, 3, 5, 6, \text{II}, \text{III}, \text{V}, \text{VI}$ ), is equal to the difference in energy required to assemble the solute charges from infinity in the two phases, A and B, where A and B are vacuum, water or liquid alkane:

$$\Delta G_j^{\text{elect}} = \frac{1}{2} \sum_i q_i (\phi_i^{\text{B}} - \phi_i^{\text{A}}) \quad (6)$$

where  $q_i$  and  $\phi_i$  are the atomic charges and calculated potentials at the  $i$ th grid point. Alternatively, the potentials across the solute-solvent dielectric boundary can be translated into effective charges located at the surface which, when embedded in a uniform solute dielectric, reproduce the reaction field, or the effect of the solvent relative to uniform solute dielectric.<sup>62</sup> The electrostatic solvation free energy is then calculated through the change in interaction energy of the solute charges with the surface charges:

$$\Delta G_j^{\text{elect}} = \frac{1}{2} \sum_{i,\sigma} \frac{q_i (q_\sigma^{\text{B}} - q_\sigma^{\text{A}})}{\epsilon_{\text{in}} r_{i\sigma}} \quad (7)$$

where  $q_i$  are the fixed charges of the solute placed at the atomic nuclei,  $q_\sigma$  represents the induced surface charges,  $\epsilon_{\text{in}}$  is the solute dielectric constant, and  $r_{i\sigma}$  are the distances between the atomic and effective surface charges. In the solvation free energy calculations presented here, the surface charge representation (eq 7) was used.

The DelPhi runs were performed at resolutions of 4 grids/Å. The electrostatic contribution to the solvation energies for molecules of the size studied here are precise to within 0.2 kcal/mol with variation of the grid scale between 2 and 5 grids/Å; thus any resolution within this range is acceptable.

**Nonpolar (Cavity/van der Waals) Solvation Free Energy Contribution,  $\Delta G_j^{\text{np}}$ .** As in previous work,<sup>55,56,63-65</sup> the nonpolar component was assumed to be proportional to the accessible surface area. Specifically, nonpolar contributions to the free energy,  $\Delta G_j^{\text{np}}$  ( $j = 2, 3, 5, 6, \text{II}, \text{III}, \text{V}, \text{VI}$ ), were calculated using the equation

$$\Delta G_j^{\text{np}} = \gamma S + b \quad (8)$$

where  $S$  is the solvent accessible surface area,  $\gamma$  is a surface area proportionality constant (sometimes referred to as a surface tension), and  $b$  is a fitted intercept.  $\gamma$  and  $b$  values of 5.5 cal/mol·Å<sup>2</sup> and 0.92 kcal/mol, respectively, were used for the vacuum to water transitions<sup>55</sup> and -27.8 cal/mol·Å<sup>2</sup> and 1.71 kcal/mol, respectively, for the water to liquid alkanes transitions.<sup>56</sup> These values were obtained from least-squares fits (standard deviations of 8% or less of the total  $\gamma$  value and 12% or less of the total value of  $b$ ) to plots of experimentally measured transfer free energies versus calculated accessible surface areas for small alkane solutes.

Equation 8 was used to calculate the nonpolar contributions to the solvation free energies of the dimer and two monomers. The nonpolar transfer energy of the two monomers is thus given by

$$\Delta G_{\text{np}}^{\text{monomers}} = 2[\gamma(S_{\text{monomer}}) + b] \quad (9)$$

An interesting issue in this procedure is whether, in the case of the dimer, the intercept  $b$  in eq 8 should contribute once or twice. If it is only counted once, the resultant net (dimer - monomers) nonpolar solvation energy would contain, in addition to a contribution due to change in surface area of the solutes upon dimerization, a contribution from the intercept, which appears twice for the two monomers but only once for the dimer. If the intercept is instead counted twice (i.e., once for each monomer in the dimer), the net nonpolar contribution returns to be simply a change in surface area, which is the more widely used function (see, e.g., Giesen et al.<sup>66</sup>). In the absence of a clear theoretical indication as to how to proceed, we have preferred the latter procedure of associating an intercept with each monomer in the dimer. We do this primarily to remain consistent with previous treatments which assume that the nonpolar contribution to dimerization is simply dependent on the change in surface area. The treatment of the intercept does not affect the hydrogen bond free energies reported in Figure 1 since the effect would in any case be subtracted out in an analogous fashion to that used in removing the effects of non-hydrogen bonding groups.

Accessible surface areas were calculated using a surface area program<sup>67</sup> which implements a modified Shrake and Rupley vertex algorithm.<sup>68</sup> For internal consistency, the same solute radii used in the electrostatic calculation were used in the solvent accessible surface area calculation. A solvent probe size of 1.4 Å, which is consistent with the parameter set, was used.<sup>55,56</sup>

For the C=O,N-H nonpolar (cavity/van der Waals) solvation free energy contributions (steps 2, 3, 5, and 6 of Figure 1), the water accessible area of the C, O, N, and H atoms involved in hydrogen bonding in the NMA dimer (and those atoms in the two monomers), in the context of the full NMA monomer and dimer, was used. No intercepts were included, as only the contributions from the hydrogen bonding (or nonbonding) portions of the molecule(s) are being considered.

### 3. Results

**NMA Dimerization.** Vacuum Phase Contribution (Step I). The vacuum internal association energy for the NMA dimer in

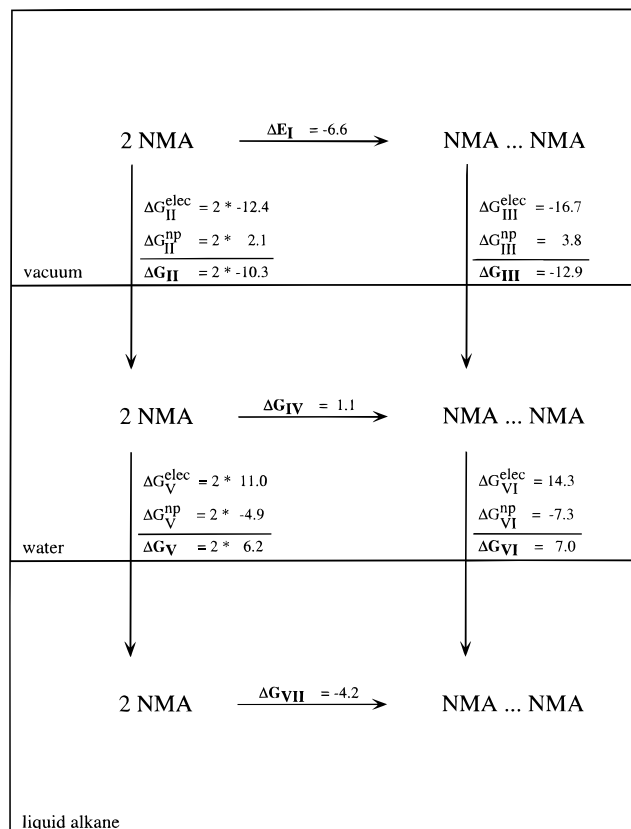


**Figure 2.** Thermodynamic cycle of the dimerization of two NMA molecules.

the overall minimized dimer conformation is  $-6.6$  kcal/mol. This value was calculated using the DGauss density functional theory program with the DZPV2 basis set and is in excellent agreement with the value of  $-6.9$  kcal/mol, which was calculated using PS-GVB, as mentioned in Theory and Methods above. Two other values have been reported in the literature:  $-6.8$  kcal/mol was calculated using GAUSSIAN 90 at the HF/6-31G\* level by Guo and Karplus,<sup>69</sup> and  $-8.9$  kcal/mol was calculated using GAUSSIAN 92 in the MP2 approximation on HF optimized geometries using the augmented CC-PVDZ basis set with no BSSE correction.<sup>70</sup> The level of those two calculations may be slightly inferior to the density functional method (and the PS-GVB).

The vacuum internal dimerization energies for the NMA dimer in  $\alpha$ -helical, parallel and antiparallel  $\beta$ -sheet conformations were also calculated using the DGauss program. The resultant energies,  $-5.5$  and  $-5.6$  kcal/mol for the  $\alpha$ -helical and the two  $\beta$ -sheet geometries, respectively, are both approximately 1 kcal/mol less favorable than for the overall minimum dimer geometry.

**Solvation Contributions (Steps II, III, V, and VI).** The electrostatic and nonpolar contribution to the solvation free energies for the NMA monomers and dimer in their minimum configuration are shown in detail in Figure 2. In Table 1, the calculated solvation free energies between water and liquid alkane are compared with other calculated and experimentally measured values for transfer from water to organic solvents; the sources of the values are described in detail in the table footnotes. As expected, due to the greater exposure of chemical groups in the two monomers relative to the dimer, in all of the methods, solvation effects are larger in magnitude for the monomers relative to the dimer (i.e., the values listed in the  $\Delta\Delta G^{w \rightarrow org}$  column in Table 1 are negative). The magnitudes of the difference vary, however, according to the various methods of estimation. The FDPB/ $\gamma$  and the Monte Carlo

**TABLE 1: Comparison of Calculated and Measured Transfer Free Energies of Hydrogen Bonding Groups between Water and Organic Solvents (kcal/mol)**

source	$\Delta G^{w \rightarrow org}$		
	two monomers	dimer	$\Delta\Delta G^{w \rightarrow org}(D-2M)$
(a) NMA/NMA			
FDPB/ $\gamma$	12.3	7.0	-5.3
Klotz et al. <sup>a</sup>	8.2	4.2, 2.7	-4.0, -5.5
Jorgensen <sup>b</sup>			-3.5
Simonson and Brunger <sup>c</sup>			-0.7
(b) N-H/C=O			
FDPB/ $\gamma$	7.8	3.8	-4.0
Klotz et al. <sup>d</sup>	4.1	0.1, -1.4	-4.0, -5.5
Roseman <sup>e</sup>	6.1	0.6	-5.5

<sup>a</sup> Experimental values for transfer from water to CCl<sub>4</sub>. Monomer transfer free energy was measured directly; the dimer value was obtained by summing monomer transfer free energy and measured association free energies in water and CCl<sub>4</sub>.<sup>9,13,27</sup> <sup>b</sup> Calculated values for transfer from water to CHCl<sub>3</sub>, obtained from difference of Monte Carlo molecular simulations of dimerization in the two solvents.<sup>28</sup> In this calculation, the water dimer minimum is observed to be in a stacked rather than hydrogen bonded geometry. <sup>c</sup> Calculated values for transfer from water to CCl<sub>4</sub>, obtained from continuum solvent model and X-PLOR forcefield.<sup>28</sup> <sup>d</sup> Monomer transfer free energy obtained by removing methyl group contributions from experimentally measured water to CCl<sub>4</sub> transfer value, using a group contribution approach; other details as in footnote a.<sup>9,13,27</sup> <sup>e</sup> Monomer transfer free energy obtained by removing methyl group contributions from experimentally measured water to CCl<sub>4</sub> transfer value, using a group contribution approach; other details as in footnote a.<sup>26</sup>

molecular simulation<sup>28</sup> methods each yield  $\Delta\Delta G^{w \rightarrow org}$  values in close agreement with one of the two values estimated based on the experimental measurements.

There are several points to note in comparing the results from the different methods. First, the organic solvent was CCl<sub>4</sub> in all of the studies excluding the FDPB/ $\gamma$  work, in which the organic solvent was liquid alkane. The greater nonpolar character of liquid alkane versus CCl<sub>4</sub> could account at least in part for the larger solvation free energies ( $\Delta G^{w \rightarrow org}$  columns in Table 1) obtained in the FDPB/ $\gamma$  versus experimental methods.<sup>56</sup>

The second point concerns the NMA dimer structure. In the FDPB/ $\gamma$  work, the dimer conformation was modeled in a hydrogen bonded form regardless of the nature of the solvent. In the Monte Carlo simulation, however, a stacked, rather than hydrogen bonded, geometry was observed to be more stable for the dimer in water. The structure of the dimer in aqueous solution measured in the experimental work<sup>9</sup> is not known. Naturally, where the structural entities being considered are not equivalent, the results can only be compared qualitatively at best.

The  $\Delta\Delta G^{w \rightarrow org}$  value obtained by Simonson and Brunger,<sup>30</sup> using continuum solvent model, is significantly smaller than all other values. The exact reason for the difference from our value, despite the fact that both methods used continuum solvent models, is difficult to follow, since the two methods are based on different parametrization schemes to reproduce the experimentally measured hydration/solvation free energies of small molecules: While we parametrized the set of atom charges and radii,<sup>55,56</sup> Simonson and Brunger parametrized the surface tension. Our parametrization scheme led to solvation free energies in a much better agreement with the measured ones (our maximum deviation, 1.2 kcal/mol, is equal to their rms deviation). In addition, after parametrizing to reproduce experimental water to cyclohexane free energies, Simonson and Brunger estimated the water to CCl<sub>4</sub> transition by setting the dielectric constant to 2.2.

**Net Dimerization Free Energies.** The NMA monomer and dimer solvation free energies have been combined with the

**TABLE 2: Comparison of Calculated and Measured Binding Free Energies of Hydrogen Bonding Groups in Water and Organic Solvents (kcal/mol)**

	$\Delta G_{\text{bind}}$		
source	water	organic solvent	$\Delta\Delta G_{\text{bind}}(\text{org-w})$
(a) NMA/NMA			
FDPB/ $\gamma$	1.1	-4.2	-5.3
Klotz et al. <sup>a</sup>	3.1	-0.92, -2.4	-4.0, -5.5
Spencer et al. <sup>b</sup>		-1.8	
Krikorian <sup>c</sup>		-1.9	
Jorgensen <sup>d</sup>	0.0	-3.5	-3.5
Simonson and Brunger <sup>e</sup>	0.6	-3.4	-4.1
(b) Other Small Molecule Dimers			
Sneddon et al. <sup>f</sup>	-0.3	-8.4	-8.1
Doig and Williams <sup>g</sup>	-3.1 to -6.2	-5.3 to -7.6	-2.2 to -0.8
Osapay et al. <sup>h</sup>	-0.8		
(c) N-H/C=O			
FDPB/ $\gamma$	-1.3	-5.3	-4.0

<sup>a</sup> Experimental values for water and CCl<sub>4</sub>.<sup>9,13,27</sup> <sup>b</sup> Experimental values for CCl<sub>4</sub>.<sup>17</sup> <sup>c</sup> Experimental values for CCl<sub>4</sub>.<sup>18</sup> <sup>d</sup> Calculated values for water and CHCl<sub>3</sub>, obtained from Monte Carlo molecular simulations of dimerization in the two solvents; the water dimer minimum is a stacked rather than hydrogen bonded geometry.<sup>28</sup> <sup>e</sup> Calculated values for water and CCl<sub>4</sub>, obtained from continuum solvent model and X-PLOR forcefield.<sup>28</sup> <sup>f</sup> Calculated values for the association of two formaldehyde molecules in water and CCl<sub>4</sub>, obtained via molecular dynamics simulation methods.<sup>29</sup> <sup>g</sup> Values extracted from experimentally measured binding constants for a range of small molecules which form hydrogen bonds in water and CCl<sub>4</sub>, by removing calculated translational and rotational entropic contributions.<sup>22</sup> <sup>h</sup> Calculated values for the association of two formaldehyde molecules in water, obtained via continuum solvent model.<sup>31</sup>

calculated vacuum dimerization energies to produce the net dimerization free energies in each solvent, as shown in Figure 2. The results indicate that the NMA dimerization process in liquid alkane is slightly less favorable relative to the vacuum phase value (-4.2 vs -6.6 kcal/mol); this is because the net solvation contribution to dimerization in liquid alkane relative to vacuum is small, but positive. The dimerization process in water is significantly less favorable than in vacuum; in fact, the water dimerization energy is +1.1 kcal/mol (opposing binding).

The experimentally measured free energies of dimerization of NMA molecule are shown in Table 2, along with several recently calculated association values for NMA/NMA as well as other molecules. The sources for the values are described in the footnotes to Table 2. In comparing the results from the different methods, there are several aspects to consider in addition to the points mentioned above in the solvation energy section. First, effects due to loss of entropy upon binding in vacuum are not included in the FDPB/ $\gamma$ , the Simonson and Brunger, the Ösapay et al., and the Doig and Williams works; in the Doig and Williams work they were subtracted from experimental values, and in the FDPB/ $\gamma$ , the Ösapay et al., and the Simonson and Brunger approach they were never considered explicitly. All other values include these entropy contributions. Entropic effects do not enter when comparing the relative free energies of association of NMA in organic solvent versus water ( $\Delta\Delta G_{\text{bind}}(\text{org-w})$ ) in the rightmost column of Table 2).

A second point is that the experimentally measured results involve some uncertainty. As shown in Table 2, different methods of measuring the NMA dimerization energy in CCl<sub>4</sub> have yielded results which differ by 1.5 kcal/mol. Finally, the zero point energies have been neglected in the FDPB/ $\gamma$  method; our estimates indicate that the net contribution of these energies to dimerization in vacuum totals approximately 1 kcal/mol.<sup>44</sup> The combined uncertainties due to the differences in organic

solvent, missing conformational entropy contributions, multiple aqueous dimer conformations, experimental variability, and use of internal energy rather than enthalpy in vacuum in the FDPB/ $\gamma$  method make it difficult to make quantitative comparisons. Overall, taking the uncertainties into account, the FDPB/ $\gamma$  energies are not in conflict with the experimental values.

Finally, notice that the FDPB/ $\gamma$  and the Simonson and Brunger methods give positive free energies of forming a hydrogen bond in water in close agreement with each other, while the third continuum solvent approach by Ösapay et al. gives a negative value. We attribute this difference to an underestimate of hydration free energies in the study of Ösapay et al., as will be discussed below.

**N-H...C=O.** We carried out natural orbital analysis for the NMA monomer and dimer in order to estimate the N-H and C=O contributions to the hydrogen bond association energy in vacuum. The total dimerization energy, -6.6 kcal/mol, is slightly larger than the energy associated with the overlap of the lone pair O and antibonding N-H orbitals, -7.6 kcal/mol, where the O, N, and H are the atoms involved in the hydrogen bond. This suggests that the dimerization energy in vacuum arises to a large extent from contributions from the hydrogen bonded atoms<sup>50</sup> although their exact contribution is difficult to determine or even unambiguously define. For simplicity we assume that the vacuum phase contribution from the hydrogen bonding N-H and C=O pair is equal to the full NMA dimerization energy.

The electrostatic solvation contributions from the N-H and C=O groups in the NMA dimer were computed by including partial charges on the hydrogen bonded N, H, C, and O atoms only; the nonpolar components were computed via the change in surface area associated with these atoms upon dimerization. The solvation contributions for the N-H/C=O groups are shown in Figure 1 and Table 1; values from previously published estimates are also included in the table for comparison. The FDPB/ $\gamma$  solvation values are smaller in magnitude than for the full NMA dimer because the contributions from the nonhydrogen bonding groups are neglected. Nevertheless, the solvation contributions remain significantly larger than previously estimated values. For example, the Roseman value for transfer of the N-H/C=O dimer was obtained by combining the experimentally measured binding free energies of NMA in water and CCl<sub>4</sub>, with the measured transfer free energy of NMA, where contributions from the methyl groups were removed using a group contribution solvation approach.<sup>26</sup> The resultant penalty for transferring the N-H/C=O dimer from water to CCl<sub>4</sub> is 0.6 kcal/mol. The energy for this process as calculated by the FDPB/ $\gamma$  method is 3.8 kcal/mol, or more than 6 times greater than Roseman's estimate. As shown in Figure 1 and Table 2, the resultant net binding energies for the N-H/C=O groups are -1.3 and -5.3 kcal/mol in water and liquid alkane, respectively.

Similar calculations were carried out for the hydration/solvation free energies of the N-H and C=O groups in the NMA monomers and dimer in the  $\alpha$ -helix and the parallel and antiparallel  $\beta$ -sheets geometries. The values that were obtained are all very similar to the ones obtained for those groups in the minimized geometry. The free energies of forming a hydrogen bond between those groups in water and liquid alkane in those geometries were estimated from the hydration/solvation values and the hydrogen bonding energies in vacuum. They are -0.5 and -0.9 kcal/mol for the  $\alpha$ -helix and the  $\beta$ -sheet geometries (both the parallel and antiparallel) in water, respectively, and -4.4 kcal/mol for the three geometries in liquid alkane.

#### 4. Discussion

Our first set of calculations for the full NMA monomers and dimer, presented in Figure 2, was carried out mainly to compare our results with previous experimental measurements and calculations.<sup>9,13,17,18,22,27-31</sup> Ideally, the organic phase in our calculations should have been CCl<sub>4</sub> or CHCl<sub>3</sub> because those are the solvents used in previous studies (see Tables 1 and 2). However, our parametrization scheme is based on a surface tension coefficient derived from the free energies of transfer of alkanes from water to liquid alkane (hexane and cyclohexane). Since to the best of our knowledge there are no experimentally measured free energies of transfer for alkanes between water and CCl<sub>4</sub> or CHCl<sub>3</sub>, we cannot derive the appropriate surface tension parameter. Hence, we cannot use those two solvents to define the organic phase. An advantage of choosing liquid alkanes as the organic phase is that they more closely resemble lipid bilayers than do CCl<sub>4</sub> or CHCl<sub>3</sub>. Taking into account this and the other complications in the comparison, our calculations, presented in Figure 2, do not seem in conflict with the values obtained on the basis of experiments, as mentioned above.

An important issue thoroughly discussed in a recent paper by Ösapay et al.<sup>31</sup> is the problem of consistency between the method used to calculate the dimerization energy in vacuum and the method used to calculate the solvation energy, when using thermodynamic cycles such as Figures 1 and 2. Ösapay et al. showed that using charges for calculating solvation energies that are larger than the charges used for calculating the dimerization (binding) energy in vacuum leads to an overestimate of the effects of solvent screening which may, in some cases, lead to a net repulsion between solute molecules that actually attract each other. They argued that since the CHARMM<sup>75</sup> charge set was parametrized to reproduce *ab initio* energies of small molecules in vacuum, it should for consistency be used for calculating the solvation energies as well. Ösapay et al. used CHARMM PARAM19 charges in conjunction with PARSE radii and an interior dielectric constant of 2. However, this procedure has its own inconsistencies; for example, the use of solute dielectric constant of 2 reduces the agreement between CHARMM and *ab initio* calculations of gas-phase dimerization energies (the calculated dimerization energy of the two NMA molecules in vacuum is reduced to -4.7, 2 kcal/mol below the *ab initio* value). Moreover, the calculated hydration free energy of the NMA monomer is only -6.0 kcal/mol, i.e., about 60% of the measured value, using the CHARMM charges, the PARSE radii and an interior dielectric of 2.

We address the issue of inconsistency of the charge sets by repeating the calculations of the thermodynamic cycle in the upper half of Figure 2 using a single set of CHARMM parameters. Recall that the CHARMM PARAM19 force field has been designed to reproduce *ab initio* calculations. Indeed the NMA dimerization energy in vacuum obtained with CHARMM is -6.9 kcal/mol, in nearly perfect agreement with our quantum chemistry calculations. To reproduce the measured free energy of hydration of the NMA monomer using the CHARMM charges with an interior dielectric of 2, we reduced all the CHARMM radii by 0.29 Å. This yields a dimerization energy of +1.7 kcal/mol in water, a value very similar to the one we calculated using the original PARSE parameters in Figure 2. Similarly, to reproduce the measured free energy of hydration of the NMA monomer using the CHARMM charges with an interior dielectric of 1, we reduced all the CHARMM radii by 0.18 Å. This gives a dimerization energy of +1.9 kcal/mol in water, again a very similar value to the one reported in Table 2. The dual requirement of maintaining consistency in charge sets and calculating accurate hydration free energies can be met by changing radii so as to reproduce hydration free energies while requiring that the charges used in the solvation calculations be consistent with those used to obtain gas-phase

dimerization energies. For the specific problem under consideration in this work, it is encouraging that very similar results are obtained with different parametrizations. The negative NMA dimerization free energy in water obtained by Ösapay et al. (as opposed to the positive one obtained here) appears to be due to their underestimate of hydration free energies due to their use of CHARMM charges and a solute dielectric constant of 2.

The free energy associated with hydrogen bond formation in water obtained in this work is -1.3 kcal/mol (Figure 1). This value is more negative than the free energy of NMA dimerization +1.1 kcal/mol (Figure 2), which also includes interactions between non-hydrogen bonded groups. The value reported in Figure 1 does not include entropic effects which will be quite sensitive to the system under study (i.e., they are different in  $\alpha$ -helix formation than in NMA dimerization). We observed no energy preference for hydrogen bonds in  $\alpha$ -helical, parallel, or antiparallel  $\beta$ -sheet geometries in the aqueous phase or in liquid alkane. Our calculations also indicate that the gas phase  $\alpha$ -helix and  $\beta$ -sheet hydrogen bond energies are practically identical. These results are in conflict with those reported by Mitchell and Price<sup>39</sup> for the amide hydrogen bond in a formamide/formaldehyde complex. They observed, for example, that a hydrogen bond in an  $\alpha$ -helix geometry is  $\sim 1.5$  kcal/mol weaker than in the parallel  $\beta$ -sheet geometry. The absolute values are also different. We have no explanation for the discrepancy between the two sets of calculations. We note that Mitchell and Price used a perturbation approach for the calculation of intermolecular forces, while in this work, a direct calculation of binding energies was carried out.

To evaluate the contribution of hydrogen bond formation to protein stability we use the thermodynamic cycle of Figure 1 where the unfolded state is represented by the isolated N-H and C=O groups in water while the folded state is represented by the N-H $\cdots$ O=C hydrogen bonded pair in liquid alkane (see, for example, Yang and Honig<sup>71</sup> for a discussion of this model). The net contribution to protein stability due to formation and burial of a hydrogen bond in the protein interior can be obtained from the free energy associated with step 8 (Figure 1). The calculated value of 2.5 kcal/mol indicates that the formation and burial of a hydrogen bond opposes protein folding. If one of the partners in a hydrogen bonded pair is removed, as has been done in several experiments,<sup>23</sup> the energy of step 5 will be approximately one-half its previous value of 7.8 kcal/mol and the energy of step 7 will be 0, since no hydrogen bond is formed. The resultant energy for step 8 is 3.6 kcal/mol. The net calculated change in stability due to the removal of a hydrogen bond partner is thus 1.1 kcal/mol, in close agreement with measured values (see the discussion in Yang and Honig<sup>71</sup>). The results obtained here also support previous work from this lab that suggests that hydrogen bonds oppose  $\alpha$ -helix formation.<sup>35,71</sup>

Step 6 of Figure 1 may be interpreted as the penalty associated with removing a hydrogen bonded pair that is exposed in water to a low-dielectric environment such as a membrane or protein interior. The result for this energy obtained using the FDPB/ $\gamma$  method, 3.8 kcal/mol, is significantly larger than previous estimates.<sup>26,27</sup> This suggests that the penalty associated with burying hydrogen bonds is significant and will have to be overcome by other energetically favorable terms (such as nonpolar contributions) if protein folding or membrane insertion is to be achieved (see discussion in Yang and Honig<sup>71</sup> and in Ben-Tal et al.<sup>72</sup>).

Many attempts have been made in the past to develop polarity (hydropathy) scales that indicate the relative tendencies of the amino acids to be inserted into lipid bilayers (see, for example, Engelman et al.<sup>73</sup> and Fasman and Gilbert<sup>74</sup>). The scales are based on the implicit assumption that each side chain has a fixed free energy contribution regardless of its neighbors and that,

by adding the contribution of the backbone, it is possible to estimate the total free energy of transfer of the amino acid. However, this assumption will not in general be correct since transfer free energies are context dependent. As an example, the free energies of transfer of the hydrogen bonded ( $\text{N}-\text{H}\cdots\text{O}=\text{C}$ ) and nonbonded ( $\text{N}-\text{H}, \text{O}=\text{C}$ ) groups between two solvents depends quite sensitively on their environment. Water to liquid alkane free energies of transfer of 2.1 and 6.4 kcal/mol, respectively, were calculated for these groups when they were a part of an  $\alpha$ -helix.<sup>72</sup> These values are  $\sim 1.5$  kcal/mol less negative than the ones reported in Figure 1, obtained when the groups were in the context of an NMA monomer and dimer. The reason for the difference is that NMA and the helix form differently shaped cavities in the solvent. Specifically, the amide groups in an  $\alpha$ -helix are surrounded by a low-dielectric region even in the aqueous phase, such that their free energies of transfer into liquid alkane are smaller than in NMA. The same logic would dictate that the transfer free energies of amino acid side chains that are part of an  $\alpha$ -helix are different than those of the isolated amino acids. The situation is compounded by the possibility of side chain–side chain and side chain–backbone hydrogen bonding interactions. It may be possible, however, to take these effects into account in devising context-dependent hydrophobicity scales.

**Acknowledgment.** We would like to thank David Chasman and Jan Lundell for helpful discussions and comments regarding the vacuum calculations and S. Sridharan for software management. Support from the NSF (MCB-9304127) and NIH (P41 RR06892) grants is gratefully acknowledged. We thank the staff and administration of Frederick Biomedical Supercomputing Center for their support of this project. The content of this paper does not necessarily reflect the views or policies of the Department of Health and Human Services, nor does mention of trade names, commercial products, or organizations imply endorsement by the U.S. Government.

## References and Notes

- (1) Baker, E. N.; Hubbard, R. E. *Prog. Biophys. Mol. Biol.* **1984**, *44*, 97–179.
- (2) Dill, K. A. *Biochemistry* **1990**, *29*, 7133.
- (3) Popot, J.-L.; Engelman, D. M. *Biochemistry* **1990**, *29*, 4031–4036.
- (4) Jeffrey, G. A.; Saenger, W. *Hydrogen bonding in biological structures*; Springer-Verlag: Berlin, 1991.
- (5) Stickle, D. F.; Presta, L. G.; Dill, K. A.; Rose, G. D. *J. Mol. Biol.* **1992**, *226*, 1143–1159.
- (6) Schellman, J. A. *Trav. Lab. Carlsberg, Ser. Chim.* **1955**, *29*, 230–259.
- (7) Schellman, J. A. *Trav. Lab. Carlsberg, Ser. Chim.* **1955**, *29*, 223–229.
- (8) Lord, R. C.; Porro, T. J. Z. *Elektrochem.* **1960**, *64*, 672–676.
- (9) Klotz, I. M.; Franzen, J. S. *J. Am. Chem. Soc.* **1962**, *84*, 3461–3466.
- (10) Franzen, J. S.; Stevens, R. E. *Biochemistry* **1963**, *2*, 1321.
- (11) Afsprung, H. E.; Christian, S. D.; Worley, J. D. *Spectrochim. Acta, Part A* **1964**, *20*, 1451–1420.
- (12) Susi, H.; Timasheff, S. N.; Ard, J. S.; Koput, J. *J. Biol. Chem.* **1964**, *239*, 3051–3054.
- (13) Kreshek, G. C.; Klotz, I. M. *Biochemistry* **1969**, *8*, 8–12.
- (14) Gill, S. J.; Noll, L. J. *Phys. Chem.* **1972**, *76*, 3065–3068.
- (15) Hopmann, R. F. W. *J. Phys. Chem.* **1974**, *78*, 2341–2348.
- (16) Josefiak, C.; Schneider, G. M. *J. Phys. Chem.* **1979**, *83*, 2126–2128.
- (17) Spencer, J. N.; Garrett, R. C.; Mayer, F. J.; Markle, J. E.; Powell, C. R.; Tran, M. T.; Berger, S. K. *Can. J. Chem.* **1980**, *58*, 1372–1375.
- (18) Krikorian, S. E. *J. Phys. Chem.* **1982**, *86*, 1975–1981.
- (19) Eberhardt, E. S.; Raines, R. T. *J. Am. Chem. Soc.* **1994**, *116*, 2149–2150.
- (20) Wimley, W. C.; Creamer, T. P.; White, S. H. *Biochemistry* **1996**, *35*, 5109–5124.
- (21) Ben-Naim, A. *J. Phys. Chem.* **1991**, *95*, 1437–1444.
- (22) Doig, A. J.; Williams, D. H. *J. Am. Chem. Soc.* **1992**, *114*, 338–343.
- (23) Fersht, A. R.; Shi, J.-P.; Knill-Jones, J.; Lowe, D. M.; Wilkinson, A. J.; Blow, D. M.; Brick, P.; Carter, P.; Waye, M. M. Y.; Winter, G. *Nature* **1985**, *314*, 235–238.
- (24) Fersht, A. R. *TIBS* **1987**, *12*, 301–304.
- (25) Shirley, B. A.; Stanssens, P.; Hahn, U.; Pace, C. N. *Biochemistry* **1992**, *31*, 725–732.
- (26) Roseman, M. *J. Mol. Biol.* **1988**, *201*, 621–623.
- (27) Klotz, I. M.; Farnham, S. B. *Biochemistry* **1968**, *7*, 3879–3832.
- (28) Jorgensen, W. L. *J. Am. Chem. Soc.* **1989**, *111*, 3770–3771.
- (29) Sneddon, S. F.; Tobias, D. J.; Brooks, C. L., III. *J. Mol. Biol.* **1989**, *209*, 817–820.
- (30) Simonson, T.; Brunger, A. T. *J. Phys. Chem.* **1994**, *98*, 4683–4694.
- (31) Ösapay, K.; Young, W. S.; Bashford, D.; Brooks, C. L.; Case, D. C. *J. Phys. Chem.* **1996**, *100*, 2698–2705.
- (32) Baldwin, R. L. *TIBS* **1989**, *14*, 291–294.
- (33) Alber, T. *Annu. Rev. Biochem.* **1989**, *58*, 765–798.
- (34) Privalov, P. L.; Makhatazde, G. I. *J. Mol. Biol.* **1993**, *232*, 660–679.
- (35) Honig, B.; Yang, A.-S. *Adv. Protein Chem.* **1995**, *46*, 27–58.
- (36) Brünger, A. T. *X-PLOR Manual*, Version 3.0; Yale University: New Haven, CT, 1992.
- (37) Warshel, A. *Computer modeling of chemical reactions in enzymes and solutions*; John-Wiley & Sons, Inc.: New York, 1991.
- (38) Hagler, A. T.; Huler, E.; Lifson, S. *J. Am. Chem. Soc.* **1973**, *96*, 5319–5327.
- (39) Mitchell, J. B. O.; Price, S. L. *J. Comput. Chem.* **1990**, *11*, 1217–1233.
- (40) Godbout, N.; Salahub, D. R.; Andzelm, J.; Wimmer, E. *Can. J. Chem.* **1992**, *70*, 560–571.
- (41) Sule, P.; A. Nagy. *J. Chem. Phys.* **1996**, *104*, 8524–8534.
- (42) Sim, F.; St-Amant, A.; Papai, I.; Salahub, D. R. *J. Am. Chem. Soc.* **1992**, *114*, 4391–4400.
- (43) Kieninger, M.; Suhai, S. *Int. J. Quantum Chem.* **1994**, *52*, 465–478.
- (44) Topol, I. A.; Burt, S. K.; Rashin, A. A. *Chem. Phys. Lett.* **1995**, *247*, 112–119.
- (45) Del Bene, J. E.; Person, W. B.; Szczepaniak, K. *J. Phys. Chem.* **1995**, *99*, 10705–10707.
- (46) Novoa, J. J.; Sosa, C. *J. Phys. Chem.* **1995**, *99*, 15837–15845.
- (47) Han, W.-G.; Suhai, S. *J. Phys. Chem.* **1996**, *100*, 3942–3949.
- (48) Dykstra, C. E. *Chem. Rev.* **1993**, *93*, 2339.
- (49) Frisch, M.; Trucks, G.; Head-Gordon, M.; Gill, P.; Wong, P.; Foresman, M.; Johnson, J.; Schlegel, H.; Robb, M.; Replogle, E.; Gomperts, R.; Andrew, J.; Ragavachari, K.; Binkley, S.; Gonzales, C.; Martin, R.; Fox, D.; Defrees, D.; Baker, J.; Stewart, J.; Pople, J. Gaussian, Inc., Pittsburgh, PA, 1992.
- (50) Reed, A. E.; Curtiss, L. A.; Weinhold, F. *Chem. Rev.* **1988**, *88*, 899–926.
- (51) Weinhold, F.; Carpenter, J. E., Eds. *The structure of small molecules and ions*. Plenum: New York, 1988.
- (52) Ringnalda, M. N.; Langlois, J.-M.; Greeley, B. H.; Russo, T. V.; Muller, R. P.; Marten, B.; Won, Y.; Donnelly, R. E., Jr.; Pollard, W. T.; Miller, G. H.; Goddard, W. A. I.; Friesner, R. A. Schrodinger, Inc., Pasadena, CA, 1993.
- (53) Friesner, R. *Annu. Rev. Phys. Chem.* **1991**, *42*, 341–362.
- (54) Dunning, T. *J. Chem. Phys.* **1989**, *90*, 1007–1023.
- (55) Sitkoff, D.; Sharp, K. A.; Honig, B. *J. Phys. Chem.* **1994**, *98*, 1978–1988.
- (56) Sitkoff, D.; Ben-Tal, N.; Honig, B. *J. Phys. Chem.* **1996**, *100*, 2744–2752.
- (57) Lide, D. R., Ed. *CRC Handbook of Chemistry and Physics*; CRC Press: Boca Raton, FL, 1992.
- (58) Sharp, K.; Jean-Charles, J.; Honig, B. *J. Phys. Chem.* **1992**, *96*, 3822–3828.
- (59) Warwicker, J.; Watson, H. C. *J. Mol. Biol.* **1982**, *157*, 671.
- (60) Nicholls, A.; Honig, B. *J. Comput. Chem.* **1991**, *12*, 435–445.
- (61) Nicholls, A.; Sharp, K. A.; Honig, B. *DelPhi*; in: *Biochemistry and Molecular Biophysics*; Columbia University, NY, 1990.
- (62) Jackson, J. D. *Classical Electrodynamics*; John Wiley and Sons: New York, 1962.
- (63) Chothia, C. *J. Mol. Biol.* **1976**, *105*, 1–14.
- (64) Hermann, R. B. *J. Phys. Chem.* **1972**, *76*, 2754–2759.
- (65) Nozaki, Y.; Tanford, C. H. *J. Biol. Chem.* **1971**, *246*, 2211.
- (66) Giesen, D. J.; Cramer, C. J.; Truhlar, D. G. *J. Phys. Chem.* **1995**, *99*, 7137–7146.
- (67) Sridharan, S.; Nicholls, A.; Honig, B. *Biophys. J.* **1992**, *61*, A174.
- (68) Shrake, A.; Rupley, J. A. *J. Mol. Biol.* **1973**, *79*, 351–371.
- (69) Guo, H.; Karplus, M. *J. Phys. Chem.* **1994**, *98*, 7104–7105.
- (70) Dixon, D. A.; Dobbs, K. D.; Valentini, J. J. *J. Phys. Chem.* **1994**, *98*, 13435–13439.
- (71) Yang, A.-S.; Honig, B. *J. Mol. Biol.* **1995**, *252*, 351–365.
- (72) Ben-Tal, N.; Ben-Shaul, A.; Nicholls, A.; Honig, B. *Biophys. J.* **1996**, *70*, 1803–1812.
- (73) Engelman, D. M.; Steitz, T. A.; Goldman, A. *Annu. Rev. Biophys. Chem.* **1986**, *15*, 321–353.
- (74) Fasman, G. D.; Gilbert, W. A. *TIBS* **1990**, *15*, 89–92.
- (75) Brooks, B. R.; Brucoleri, R. E.; Olafson, B. D.; States, D. J.; Swaminathan, S.; Karplus, M. *J. Comput. Chem.* **1983**, *4*, 187–217.